Bull. Inst. Chem. Res., Kyoto Univ., Vol. 72, No. 5-6, 1995

REVIEW

Comparative Studies on Folded-Chain Structures of Polyethylene and Cycloparaffin Crystals Grown from Solutions

Masaki TSUJI*,† and Kyo Jin IHN**

Received December 5, 1994

The fold surfaces of solution-grown single crystal platelets of linear polyethylene [PE] and of some cycloparaffins such as $(CH_2)_{36}$, $(CH_2)_{60}$ and $(CH_2)_{120}$ were decorated with vapor-deposited PE. The TEM micrographs of and their corresponding electron diffraction patterns from such surface-decorated single crystals demonstrated that the surface of PE single crystal is ordered enough to define the avarage direction of folding, but not so fully regular as those of the cycloparaffins.

Edge-on crystals of PE and $(CH_2)_{120}$ were epitaxially grown from respective solutions onto the (001) face of NaCl, and then their dark-field images were obtained by TEM. Negative staining of them with RuO_4 was also performed, to estimate their lamellar thicknesses. The results suggested that there exists a "disordered" surface layer on each side of the crystalline core in a PE single crystal. The surface layer is, however, not so seriously disordered because the average direction of folding should be defined as mentioned above. The surface of PE single crystal, accordingly, seems to be composed of adjacent-reentrant folds with some fluctuation in contour length and its resultant fluctuation in conformation.

KEY WORDS: Polyethylene/ Cycloparaffin/ Folded-chain structure/ Fold surface/ Morphology/ Transmission electron microscopy/ Negative staining/ RuO_4/ Electron diffraction/ Surface decoration/ Epitaxy

INTRODUCTION

Polyethylene [PE] has the simplest repeating unit, $-CH_2-CH_2-$, of all the synthetic linear polymers. Accordingly, extensive studies on PE have been carried out so far as a model material representing crystallizable flexible polymers, especially to elucidate the relationship between their morphologies and physical properties. As known well broadly, the flexibility of PE chain is attributable to the relatively low energy barrier for rotation of chain segments around the carbon-carbon bonds. The chain segments which are accommodated as stems in the crystalline core of a PE crystal, of course, have the all-trans zigzag conformation (2_1 helix). Nowadays nobody doubts the existence of the folded-chain lamellar structure of PE crystals grown under ordinary conditions, *e.g.*, under an atmospheric pressure. However, many questions remain about the folding of PE chains,[1-5] such as: Is the fold surface of the crystals ordered or not?; If it is ordered, what is the detailed strucure of the fold?

* 辻　正樹: Laboratory of Polymer Condensed States, Division of States and Structures, Institute for Chemical Research, Kyoto University Uji, Kyoto-fu 611, Japan

** 印　教鎭: Department of Polymer Engineering, Dankook University, Seoul 140-714, Korea

† To whom correspondence should be addressed.

Chain folding was also reported in other flexible polymers such as polyoxymethylene and poly(4-methyl-1-pentene).[1,2] The characteristics of chain folding in these polymers are analogous to those in PE: the fold length, namely the lamellar thickness, depends on the degree of supercooling and increases by annealing.[1,2] Folded-chain crystals with a lamellar morphology can grow both from the melt and from solution. In general, crystals derived from the melts seem to be less ordered than those grown from dilute solutions. Thin lamellar crystals, namely "single crystals" of PE are usually produced by maintaining its dilute solution at a certain crystallization temperature below the dissolution temperature. Lozenge-shaped crystalline platelets grow, say below 80°C in a *p*-xylene solution, and truncated lozenge-shaped ones are formed at higher temperatures.[6]

Three different models have been proposed for the folded-chain structure of polymer

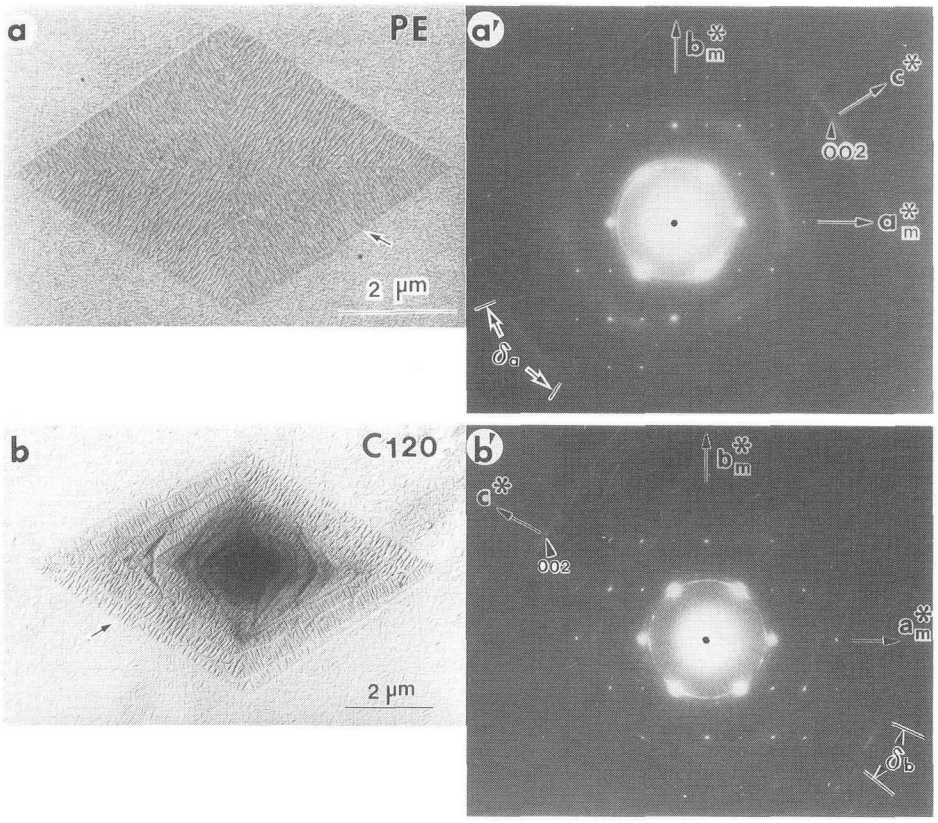

Fig. 1.
(a) PE single crystal grown from an 0.001wt% *p*-xylene solution at 80°C (decorated with vapor-deposited PE and then shadowed with Pt-Pd).
(a') ED pattern obtained from the lower-right sector indicated by the arrow in (a). The subscript *m* denotes the mother crystal (PE single crystal). $\delta_a = ca.\ 30°$.
(b) Single crystal of orthorhombic C120 grown from an 0.01wt% *p*-xylene solution at 55°C (decorated with vapor-deposited PE and then shadowed with Pt-Pd).
(b') ED pattern obtained from the lower-left sector indicated by the arrow in (b). The subscript *m* denotes the mother crystal (C120). $\delta_b = ca.\ 15°$.

single crystals:[7] 1) a regular sharp fold model[8], 2) a switch board model[9], and 3) a loose loop model[10]. A "stacked-sheets" model was also proposed for rapidly solution-crystallized samples.[11] Some regularity of fold surface of PE single crystals was derived from experimental evidence obtained by a variety of methods such as selective oxidation of the fold surfaces with fuming nitric acid,[12] obsevation of moiré patterns and/or dislocation networks produced by bilayered lamellae,[13] and infrared adsorption of mixed crystals of PE and perdeuterated PE.[14] Sectorization recognized in some polymer single crystals seems also to be a direct evidence of fairly regular fold surfaces of the crystals.[5] Wittmann and Lotz[15] inferred a regular fold structure in the surfaces of PE single crystals from the fact that PE chains vapor-deposited onto PE single crystals orient parallel to each growth face which subtends to the corresponding sector of the crystals (see Figs. 1a and 5a). On the other hand, Yoon and Flory[16] proposed again the switch board model based on the analysis of neutron scattering functions for the mixed crystal of protonated and deuterated PEs, and concluded that the adjacent reentry takes place infrequently in melt-crystallized PE and nonadjacent folds are predominant even in solution-grown crystals. Nowadays, however, the picture of PE single crystal with fairly regular and sharp folds is widely believed to be the most probable.[5] Even if it is true, some problems such as the size of folds and the folding direction remain still unsolved. In this communication, the folded-chain structure of PE single crystal is discussed by comparison with that of some cycloparaffins which undoubtedly have regular sharp folds.

EXPERIMENTAL

Single crystals of fractionated PE (NBS reference material, SRM-1482/ M=13,600 and SRM-1483/ M=32,100) and some cycloparaffins ($(CH_2)_{36}$ [C36], $(CH_2)_{60}$ [C60], $(CH_2)_{120}$ [C120]) were prepared from respective solutions. Lozenge-shaped single crystals of PE (SRM-1482) were grown from an 0.001wt% solution in *p*-xylene at 80°C[17] using the self-seeding technique[18]. The single crystal platelets of C36 were grown from a *p*-xylene solution by evaporating the solvent on the carbon-coated grid for transmission electron microscopy [TEM], and those of C60 were grown isothermally at 40°C from an 0.01wt% *p*-xylene solution.[17,19,20] The lozenge-shaped single crystals of C120 were grown from an 0.01wt% *p*-xylene solution at 55°C.[17,20,21] The truncated single crystals of PE (SRM-1483) were grown at 90°C from an 0.01wt% solution in *n*-octane using the self-seeding method.[22] The fold surfaces of these single crystals were decorated with vapor-deposited PE under vacuum:[15] PE used for vapor deposition was a commercial product (Sholex 6009 or 6050).[17,19-22]

Edge-on crystals (see Fig. 2b) of PE (SRM-1482) were grown isothermally at 80°C or 85°C on the newly cleaved (001) face of NaCl from an 0.01wt% *p*-xylene solution.[17,23] Edge-on crystals of C120 were also grown at 60°C on NaCl from an 0.01wt% *p*-xylene solution. Some of the dried edge-on crystals were annealed as they were on NaCl. Then, some of the edge-on crystals (PE and C120) thus prepared were stained with RuO_4.[17,21,23]

TEM of above-mentioned specimens was performed using a JEOL JEM-200CS operated at 200kV.

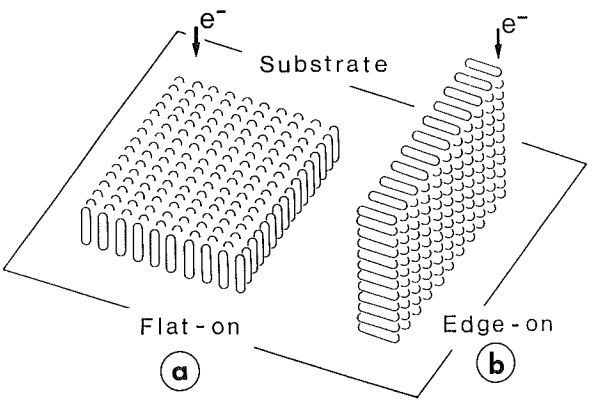

Fig. 2. Models of flat-on (a) and edge-on (b) lamellar crystals. Electron beams can be introduced normal (a) or parallel (b) to the fold surface of the crystals in transmission electron microscopy [TEM].

RESULTS AND DISCUSSION

Surface Decoration of PE and Cycloparaffin Single Crystals With Vapor-deposited PE[17,19,20,22]

When the fold surfaces of monoclinic cycloparaffin (C36, C60) single crystals were decorated with vapor-deposited PE, rod-like crystals of PE were grown with their long axis being perpendicular to the *b*-axis of the cycloparaffins (Fig. 3). Electron diffraction [ED] patterns revealed that the rods are the "edge-on" crystals of PE and its chain axis is set perpendicular to the rod axis. The chain axis of PE in a rod orients parallel to the *b*-axis, *i.e.*, the folding direction of the cycloparaffins:[19,20] calculation of adsorption energy also explained well the observed orientation of PE chains vapor-deposited onto C36 whose fold structure is fully known,[24] and it is deduced that the crystal structure of C60 is similar to that of C36.[20,25,26]

On the basis of the surface decoration of PE single crystal (Figs. 1a and 1a'), the deposited PE chains orient parallel to the (110) growth face in every (110) sector of a lozenge-shaped single crystal of PE (SRM-1482; M =13,600), and it is concluded that the (110) fold is dominant in such a sector. Figure 4 shows the relation between the chain axis of vapor-deposited PE and the folding direction in the (110) sector of PE single crystal.[20] As shown in Fig. 5, the PE chains also orient parallel to the (100) growth face in each (100) sector of a truncated single crystal of PE (SRM-1483; M=32,100). This result indicates that the (100) fold is dominant in the (100) sectors of PE single crystals. It is, therefore, concluded that PE single crystals have fairly ordered fold surfaces. Our results mentioned above of surface decoration of C36 and C60 with vapor-deposited PE strongly supported this conclusion which had been made before by Wittmann and Lotz[15]. In decorated PE single crystals, however, the 002 reflection of deposited PE is rather arc-shaped (see Figs. 1a' and 5b). The azimuthal angle δ of the reflection, which angle shows the angular distribution of the c^*-axis of the vapor-deposited PE crystals in the ED pattern, is estimated as follows: $\delta_a = ca.\ 30°$ for the (110) sector of the lozenge-shaped single crystal (Fig. 1a'); δ_A, $\delta_B = ca.\ 28°$ for the (100) and (110) sectors of the truncated one, respectively (Fig. 5b). On the other hand, the 002 reflection in

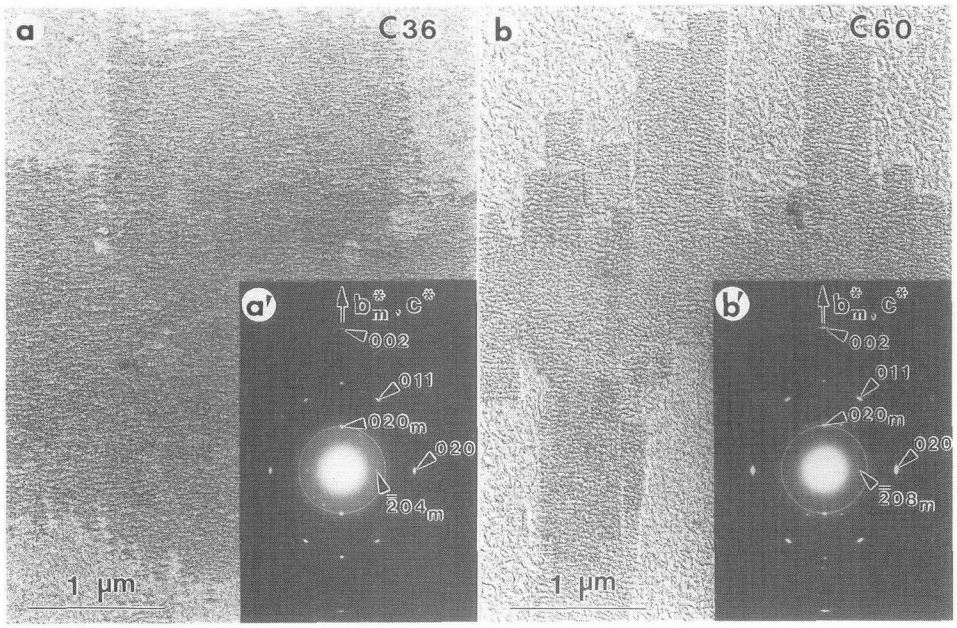

Fig. 3. Single crystals of C36 (a) and C60 (b) decorated with vapor-deposited PE (shadowed with Pt-Pd), and their ED patterns (a') and (b'), respectively. The subscript *m* denotes the mother crystals (C36 in (a') and C60 in (b')). Here, newly defined unit cells[17,20,26] of C36 and C60 were used for indexing the reflections in (a') and (b'). The PE chains orient in the direction of *b*-axis of C36 and C60, which fact shows the folding direction is in the *b*-axis direction (vertical in Fig. 3) in both C36 and C60.

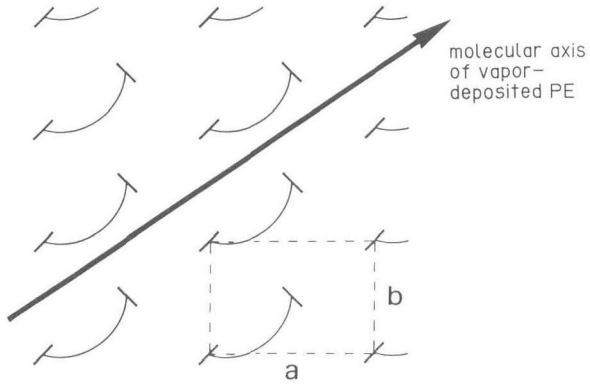

Fig. 4. Schematic representation of the orientation of vapor-deposited PE chains on the (110) sector of the single crystals of PE and orthorhombic C120. This orientation was well confirmed by energy computation on the basis of a possible model of regular fold surface for the (110) sector of PE.[38]

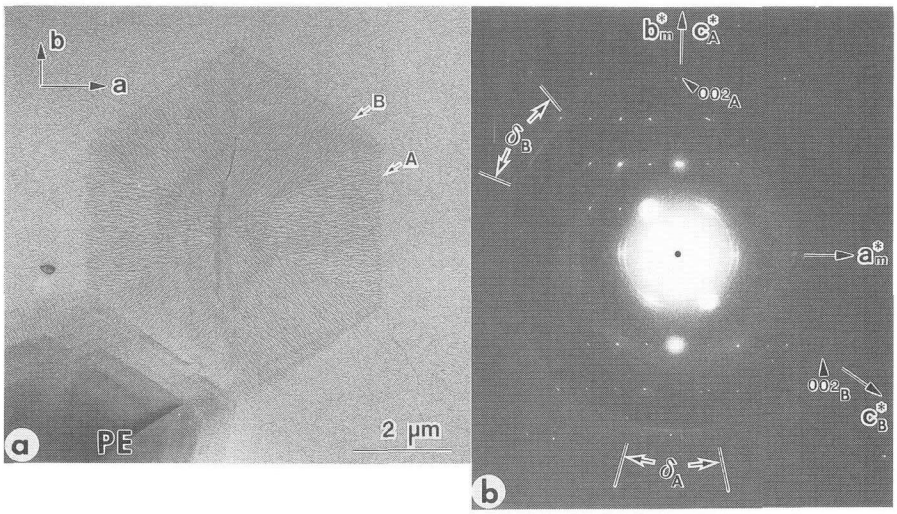

Fig. 5.
(a) PE single crystal grown from an 0.01wt% *n*-octane solution at 90°C (decorated with vapor-deposited PE, and then shadowed with Pt-Pd).
(b) ED pattern obtained from both the upper-right sector (B: (110) sector) and the right one (A: (100) sector) in (a). The subscript *m* denotes the mother crystal (PE single crystal). The subscripts *A* and *B* correspond to the sectors A and B in (a), respectively. Both δ_A and δ_B are *ca.* 28°.

question from decorated C36 and C60 crystals is fairly spot-like ($\delta < 5°$; compare Figs. 3a' and 3b' with Figs. 1a' and 5b). From these observations, it is concluded that the surface of PE single crystal (of course, in both the (100) and (110) sectors) is ordered enough to define the average direction of folding,[20] but not so fully regular as that of C36 and C60.

Edge-on Crystals of PE Grown on NaCl from Solution[17,21,23]

Figure 6 shows the morphology (a) of PE edge-on crystals grown isothermally at 80°C on NaCl, its corresponding ED pattern (b), and the dark-field image (c, d) which was taken using the 002 reflection indicated by the arrowhead in the vertical direction of Fig. 6b. As shown in Fig. 6a, rod-like crystal blocks are oriented in the 〈110〉 directions of NaCl. Figure 7a shows the PE edge-on crystals thus grown and then stained with RuO_4. A few fine dark striations due to RuO_4 can be seen as running parallel side by side between two thick striations: RuO_4 permeated into the edge-on crystal block (fine striations) and also was deposited fairly heavily on both lateral sides of the block (thick striations). The parallel fine striations owing to staining indicate that an edge-on crystal block of 20-40 nm in width consists of several edge-on lamellae. The average distance (13 nm) between the adjoining fine striations was regarded as the lamellar thickness of PE crystals grown at 80°C in a *p*-xylene solution.[23] In the 002 dark-field image (Fig. 6c), fine bright striations running in the horizontal direction are observed: this result directly shows that the chain axis of PE is normal to the long axis of the crystal blocks. As shown in Fig. 6d which has reversed contrast, the width (7 nm) of "bright" striations is much smaller than the whole width of the blocks and is assigned to the

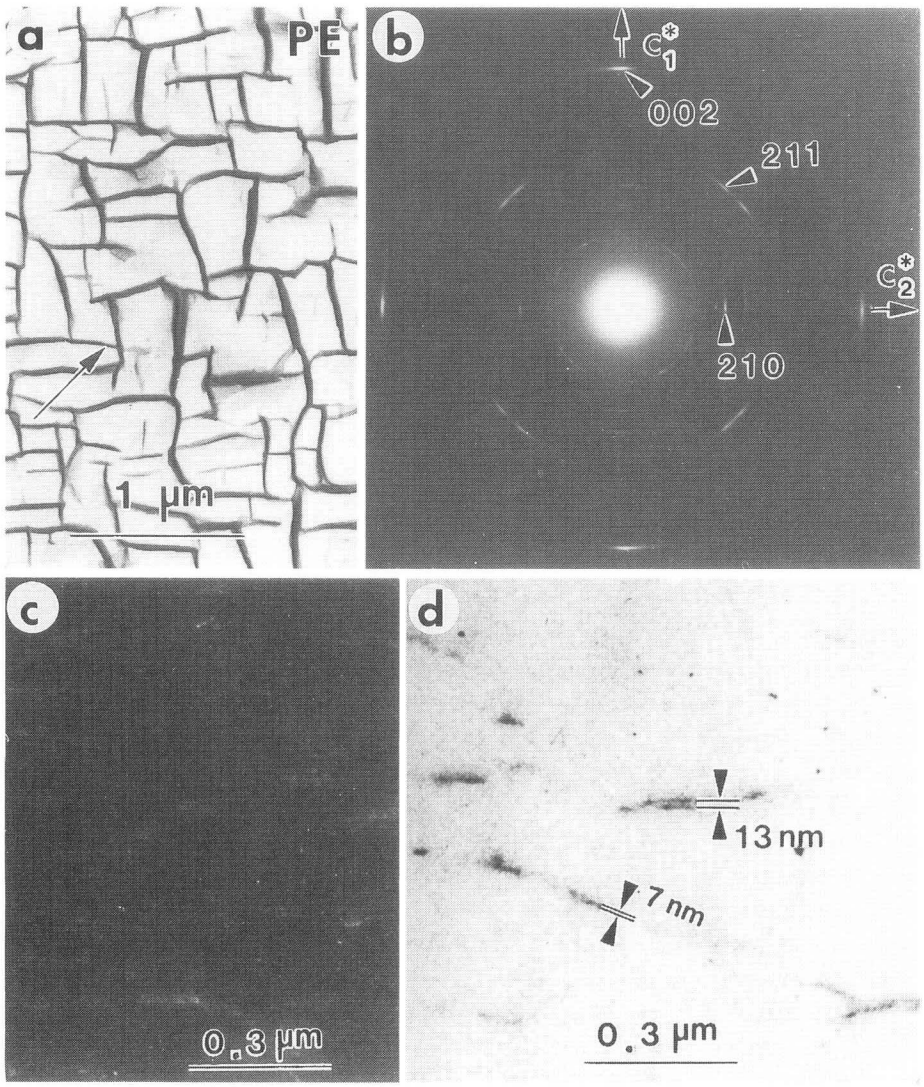

Fig. 6.
(a) Edge-on crystals of PE grown on NaCl from an 0.01wt% *p*-xylene solution at 80°C. The arrow indicates the [100] direction of NaCl, and the specimen was shadowed with Pt-Pd in this direction.
(b) Corresponding ED pattern.
(c,d) Dark-field image taken using the 002 reflection on the meridian in (b): the reflection is indicated with the arrowhead.
In an edge-on crystal, the PE chain stems are set normal to the long axis of the crystal. In (d), contrast is reversed.

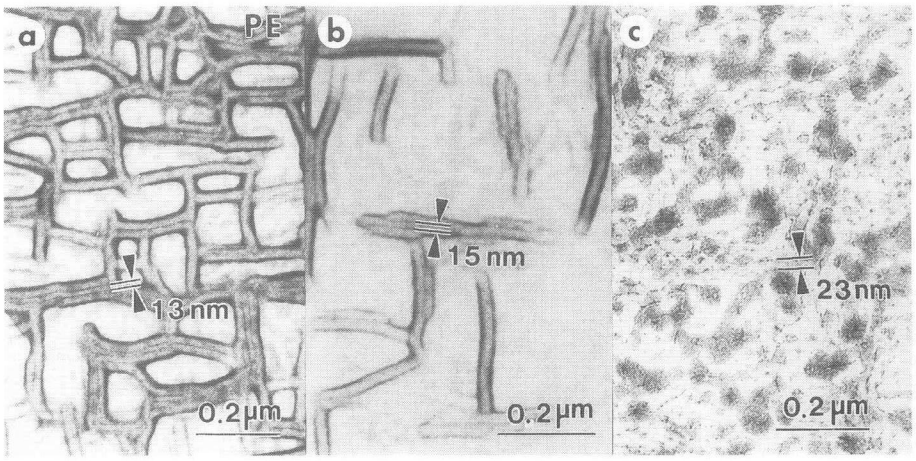

Fig. 7. Edge-on crystals of PE stained with RuO_4.
(a) Grown on NaCl at 80°C from an 0.01wt% *p*-xylene solution.
(b) Grown on NaCl at 85°C from an 0.01wt% *p*-xylene solution.
(c) Thickened crystals which were grown on NaCl at 80°C from solution and then annealed there at 120°C for 30 min after drying.

thickness of crystalline core (crystalline lamellar interior) in one edge-on lamella of PE. We recognized the fact that here and there in the original negatives, two or more striations in a crystal block run parallel side by side with a certain spacing (Fig. 6d): this spacing (13 nm) is regarded as the lamellar thickness and is equal to that estimated in the RuO_4-stained edge-on crystals (Fig. 7a). Figure 7b shows the RuO_4-stained edge-on crystals of PE which were grown on NaCl at 85°C: the lamellar thickness is estimated at about 15 nm. The thickness of 13 nm for 80°C and that of 15 nm for 85°C are almost similar to or slightly greater than the lamellar thicknesses/long periods reported in the literature[27], which were measured by TEM, and/or by small-angle X-ray scattering of the respective single crystal mats made by sedimenting single crystals grown at 80°C and at 85°C from dilute xylene solutions.

The edge-on crystals of PE grown on NaCl at 80°C were annealed on NaCl at 120°C for 30 min after drying and then stained with RuO_4 (Fig. 7c). The lamellar thickness certainly increased to 23 nm by this annealing. Figure $8a_1$ shows the morphology of PE edge-on crystals which were grown on NaCl at 80°C and then annealed there at 125°C for 60 min after drying. The ED pattern (Fig. $8a_2$) from the annealed crystals shows better orientation than that (Fig. 6b) from as-grown edge-on crystals. The 002 dark-field image (Fig. $8a_3$) of the crystals annealed at 125°C indicates that the lamellar thickness is *ca.* 36 nm and the crystalline core thickness is *ca.* 30 nm. The lamellar thickness of 23 nm for annealing at 120°C and that of 36 nm for annealing at 125°C are greater than those obtained at respective annealing temperatures in the literature.[28] Edge-on crystals of PE grown on NaCl at 80°C were heated up to 150°C after drying to be melted, and then re-crystallized at 125°C for 60 min while still on NaCl. Figure $8b_1$ shows the morphology of the crystals thus prepared. The corresponding ED pattern (Fig. $8b_2$) is similar to Fig. $8a_2$. The 002 dark-field image (Fig. $8b_3$) gives the lamellar thickness of *ca.* 42 nm and the crystalline core thickness of 32 nm, but the former

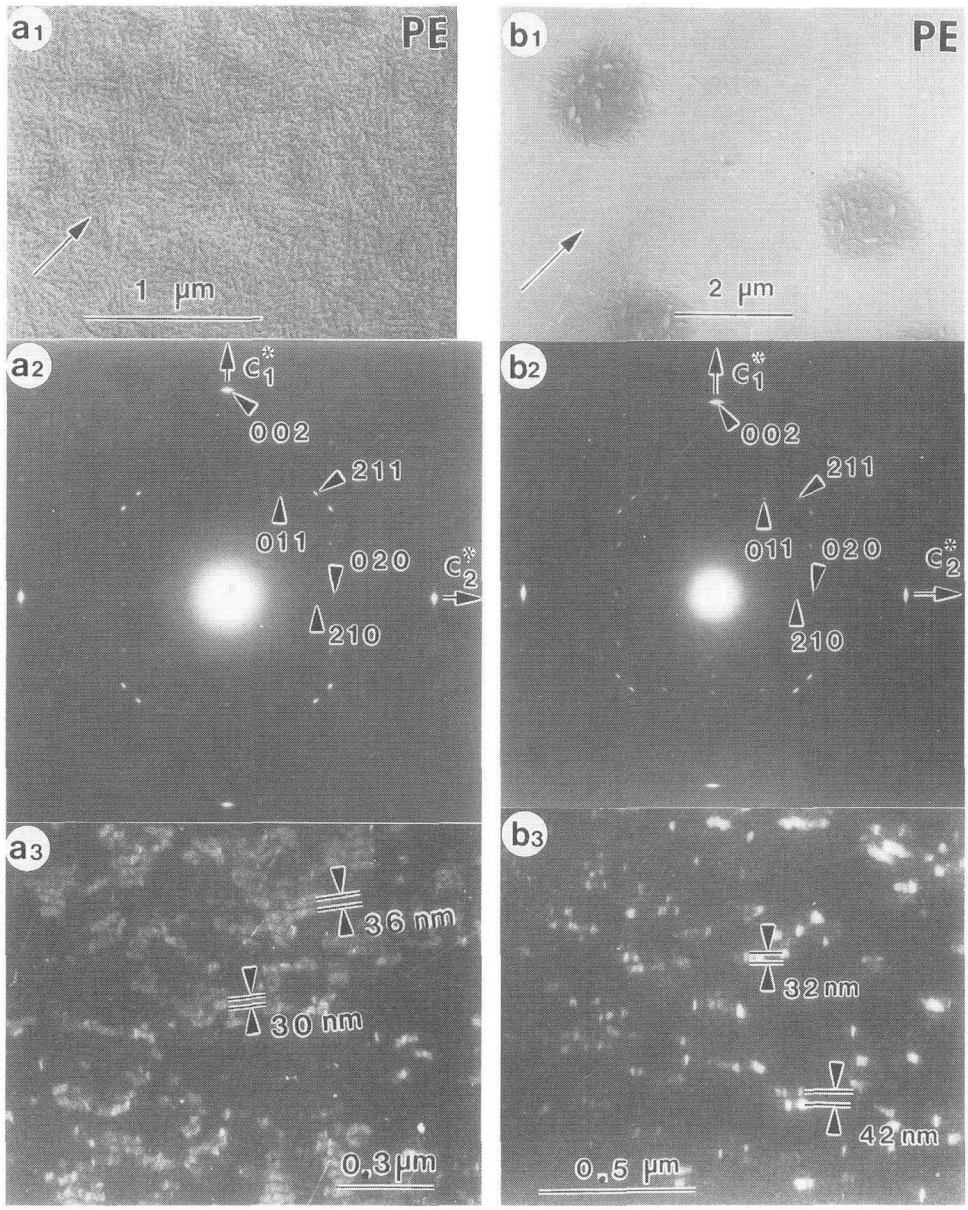

Fig. 8.
(a_1) Thickened PE edge-on crystals on NaCl by annealing at 125°C for 60 min.
(a_2): corresponding ED pattern, (a_3): 002 dark-field image.
(b_1) Melt-recrystallized PE edge-on crystals.
(b_2): corresponding ED pattern, (b_3): 002 dark-field image.
In both (a_1) and (b_1), the arrows indicate the [100] direction of NaCl, and the specimens were shadowed with Pt-Pd in this direction. In taking the dark-field images (a_3 and b_3), the 002 reflection on the meridian was used, as indicated with the arrowheads in (a_2) and (b_2).

Table 1. The average thickness of lamella and that of crystalline core estimated by various methods for PE.

crystallization or annealing temperature	average thickness (nm)					
	A	B	C	D	E	F
80°C	13	13	13	7	6	12−13
85°C	15	—	—	—	—	12−14
annealed at 120°C	23	26	26	20	6	15−20
annealed at 125°C	—	36	36	30	6	19−30
melt-recrystallized at 125°C	—	42	42	32	10	20

A: lamellar thickness estimated by staining with RuO_4.
B: lamellar thickness estimated by metal-shadowing.
C: lamellar thickness estimated from dark-field image.
D: crystalline core thickness estimated from dark-field image.
E: difference between C and D.
F: lamellar thickness cited from Refs.27 and 28.

Table 2. Sub-cell dimensions of $(CH_2)_{120}$ [C120][21]

crystal system	a (nm)	b (nm)	c_s (nm)	α (°)	β (°)	γ (°)
monoclinic	0.482	0.817	0.254	90.	90.	109.1
orthorhombic	0.746	0.498	0.254	90.	90.	90.

value is much greater than that expected from the literature[28], probably because the real crystallization temperature seems to have been higher than 125°C. The lamellar thickness and the thickness of crystalline core are summarized in Table 1[29], together with the lamellar thickness estimated by metal-shadowing and that cited from the literature.[27,28] This table also shows the difference between the lamellar thickness and crystalline core thickness which were both estimated from the same dark-field image: here, this difference is important. This table demonstrates that the difference (6 nm) in thickness was practically independent of the crystallization/annealing temperatures in our experiment. It is concluded that there are surface layers of about 3 nm thick on both sides of the crystalline core within a PE lamella. The existence of the surface layers of about 3 nm thick in the edge-on lamellae of isotactic polystyrene was also inferred from the high-resolution TEM of the thin crystalline films.[30] The thickness of surface layers for the melt-crystallized PE, however, seems to be greater than 3 nm, as shown in Fig. $8b_3$ and in Table 1.

Single Crystal of Orthorhombic C120 and Edge-on Crystals of C120[17,20,21,23,31]

Short-chain cycloparaffins such as C36 and C60 crystallize in monoclinic forms and the conformation of their folds is *-t(ggtgg)t-*.[25,26] Consequently they are not adequate as a model of folded-chain structure in orthorhombic PE. In contrast to them, C120 crystallizes with an orthorhombic sub-cell and occasionally with a monoclinic sub-cell.[21] Sub-cell dimensions of these two are shown in Table 2. They are very similar to the unit cell dimensions of

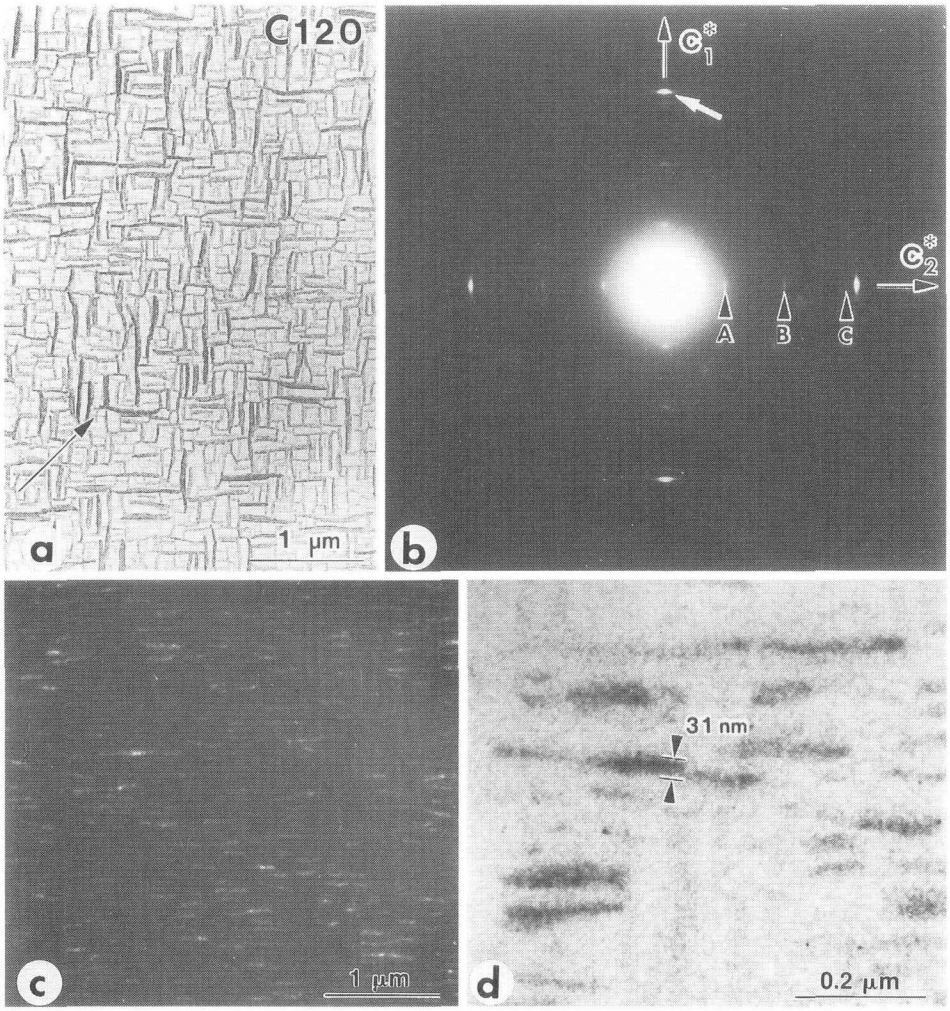

Fig. 9.
(a) Edge-on crystals of C120 grown on NaCl at 60°C from an 0.01wt% *p*-xylene solution. The arrow indicates the [100] direction of NaCl, and the specimen was shadowed with Pt-Pd in this direction. The edge-on lamellae seem to stand upright on NaCl like a wall, according to the TEM observation by specimen tilting.[31]
(b) Corresponding ED pattern.
(c) Dark-field image taken using the reflection marked with the white arrow in (b). The reflection corresponds to 002 of PE. In an edge-on crystal, the molecular axis of C120 is set normal to the long axis of the crystal.
(d) Highly enlarged from (c) with reversed contrast.

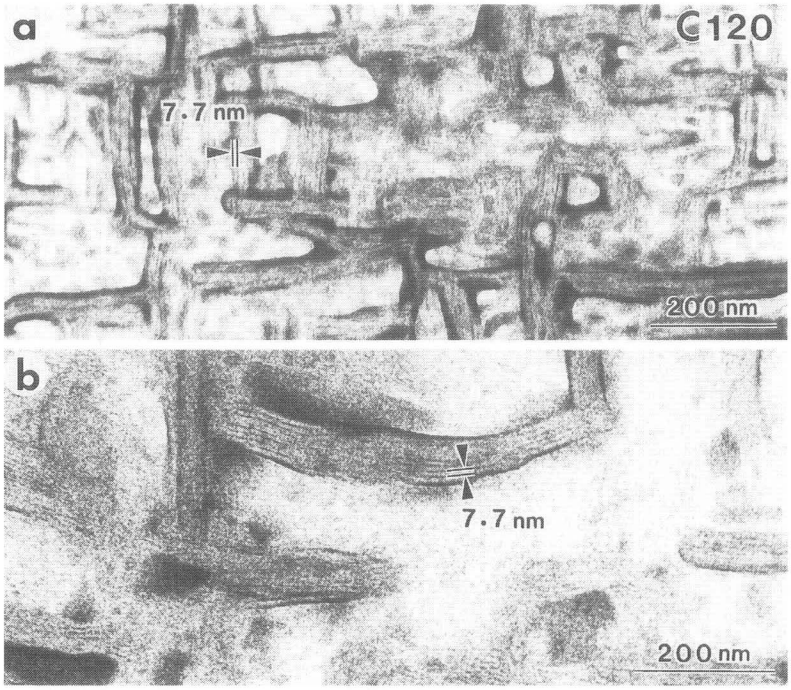

Fig. 10. Edge-on crystals of C120 stained with RuO_4.
(a) Monoclinic C120 grown at 60°C on NaCl from a *p*-xylene solution.
(b) Orthorhombic C120 transformed from the monoclinic form by annealing while still on NaCl at 110°C for 60 min after drying.

orthorhombic and monoclinic PE, respectively.[21]

The lozenge-shaped single crystal of orthorhombic C120 is very similar to that of PE in morphology, and surface decoration also reveals similar features as in a PE single crystal (Figs. 1b and 1b').[20] Thus, the orthorhombic single crystal of C120 with a lozenge-shaped lateral habit has (110) folds in each (110) sector. As shown in Fig. 1b', the 002 reflection of vapor-deposited PE on the C120 orthorhombic single crystal is arc-shaped, like that on the PE single crystal (compare Fig. 1b' with Figs. 1a' and 5b). The angle δ_b, which shows the angular distribution of the c^*-axis of deposited PE crystals, is *ca.* 15°. This value is definitely smaller than that for PE (Figs. 1a' and 5b), but rather greater than that expected from the results obtained for C36 and C60 (Fig. 3). On the other hand, the angle in question for the C120 monoclinic single crystal decorated with vapor-deposited PE was smaller than 5°,[21] which fact is analogus to C36 and C60 and indicates that the fold surface of orthorhombic C120 is less ordered than that of monoclinic C120. The 002 arc-shaped reflection of the deposited PE on orthorhombic C120 was, in our previous paper[20], attributed to the fact that the purity of the sample is about 90%, the impurities of which are mainly $(CH_2)_{108}$ and $(CH_2)_{132}$. The monoclinic single crystal, however, is assumed to be composed of pure $(CH_2)_{120}$, and accordingly to give better orientation of deposited PE chains than the orthorhombic one.

Figure 9a is the edge-on crystals of C120 which were grown on NaCl at 60°C, showing the

similar texture to that in Fig. 6a. The corresponding ED pattern (Fig. 9b) indicates that the molecular axis of C120 is oriented in the ⟨110⟩ directions of NaCl because the reflections corresponding to 002 of PE appear in these directions. The crystal form of these as-grown edge-on crystals is, however, monoclinic, judging from appearance of the reflections marked with the letters A, B and C.[21,31] According to the TEM observation of these edge-on crystal blocks by tilting, the blocks seem to stand upright on NaCl like a wall.[31] The as-grown monoclinic form of C120 was transformed while still on NaCl into the orthorhombic one by annealing.[21] Staining of C120 edge-on crystal blocks with RuO_4 clearly visualized the stacked lamellar structure in the blocks (Fig. 10).[21,23] The spacing (7.7 nm) between parallel dark striations corresponds to the molecular length of C120, namely to the thickness of mono-molecular layer in both of the monoclinic and orthorhombic forms, as demonstrated in Fig. 10. Thus, the crystallographic *c*-dimensions for both forms were assumed to be 7.7 nm.[21,31] The dark-field images of edge-on crystals of monoclinic C120 taken using the reflection corresponding to 002 of PE, however, do not show any fine striations in the edge-on crystal blocks of C120: the width of bright band in Fig. 9c is practically identical to the whole width of the block (see also Fig. 9d).[21] This fact is easily understood because the fold surface of cycloparaffins is expected to be much more regular than that of PE.

CONCLUSING REMARKS

There exist surface layers on both sides of the crystalline core in a PE single crystal. The core gives the 002 reflection, while the surface layer including folds makes a small or no contribution to the reflection due to, probably, its disorder. The surface is, however, not so seriously disordered as that of a switch board model because the average direction of folding can be defined in a PE single crystal. Consequently, the surface seems to be composed, basically, of adjacent-reentrant folds, which have, however, some fluctuation in contour length and its resultant fluctuation in conformation.[17,32] The solid-state ^{13}C NMR study on the phase structure of PE crystal suggests that the solution-grown PE crystal is composed of the crystalline core and the noncrystalline interfacial component with no rubbery contribution.[33] The component seems to be attributable to the surface layer mentioned above.

Recently, scanning probe microscopy such as atomic force microscopy [AFM] of the fold surface of PE single crystal was reported, showing that the surface is fairly regular, in particular in the directionality of folding.[34,35] A similar result was also obtained for the polyoxymethylene single crystal.[36] Individual chains and a hairpin chain fold were visualized in the "atomic-level" AFM image of highly oriented PE.[37] In the near future, therefore, a clear picture of the fold surface in PE single crystals will be given by such new techniques.

REFERENCES

(1) P. H. Geil, "Polymer Single Crystals", Robert E. Krieger Pub., Huntington (1973).
(2) B. Wunderlich, "Macromolecular Physics", vol.1, Academic Press, New York (1973).
(3) F. Khoury and E. Passaglia, in "Treatise on Solid State Chemistry", vol.3, ed. by N. B. Hannay, Plenum Press, New York, Chapt.6, pp.335-496 (1976).
(4) "Organization of Macromolecules in the Condensed Phase", *Faraday Disc. Chem. Soc.*, vol.68 (1979).
(5) D. C. Bassett, "Principles of polymer morphology", Cambridge Univ. Press, Cambridge (1981).

(6) T. Kawai and A. Keller, *Phil. Mag.*, **11**, 1165 (1965).
(7) I. Ando, T. Sorita, T. Yamanobe, T. Komoto, H. Sato, K. Deguchi and M. Imanari, *Polymer*, **26**, 1864 (1985).
(8) A. Keller, *Phil. Mag.*, **2**, 1171 (1957).
(9) P. J. Flory, *J. Amer. Chem. Soc.*, **84**, 2857 (1962).
(10) E. W. Fischer and R. Lorenz, *Kolloid-Z. Z. Polym.*, **189**, 97 (1963).
(11) M. Stamm, E. W. Fischer, M. Dettenmaier and P. Convert, pp.263-278 in Ref.4.
(12) T. Williams, D. J. Blundell, A. Keller and I. M. Ward, *J. Polym. Sci.: Part A-2*, **6**, 1613 (1968).
(13) V. F. Holland, *J. Appl. Phys.*, **35**, 3235 (1964); V. F. Holland and P. H. Lindenmeyer, *ibid.*, **36**, 3049 (1965); pp.469-485 in Ref.2; pp.56-61 in Ref.5.
(14) M. I. Bank and S. Krimm, *J. Polym. Sci.: Part A-2*, **7**, 1785 (1969).
(15) J. C. Wittmann and B. Lotz, *J. Polym. Sci.: Polym. Phys. Ed.*, **23**, 205 (1985).
(16) D. Y. Yoon and P. J. Flory, pp.288-296 in Ref.4.
(17) K. J. Ihn, Dissertation (Dr. of Eng.), Kyoto Univ (1990).
(18) D. J. Blundell, A. Keller and A. J. Kovacs, *J. Polym. Sci.: Part B (Polym. Letters)*, **4**, 481 (1966).
(19) K. J. Ihn, M. Tsuji, S. Isoda, A. Kawaguchi, K. Katayama, Y. Tanaka and H. Sato, *Makromol. Chem., Rapid Commun.*, **10**, 185 (1989).
(20) K. J. Ihn, M. Tsuji, S. Isoda, A. Kawaguchi, K. Katayama, Y. Tanaka and H. Sato, *Macromolecules*, **23**, 1781 (1990).
(21) K. J. Ihn, M. Tsuji, A. Kawaguchi and K. Katayama, *Microsc. Res. Tech.*, **20**, 205 (1992).
(22) A. Kawaguchi, M. Ohara and M. Tsuji, *J. Polym. Sci.: Part B: Polym. Phys.*, **32**, 421 (1994).
(23) K. J. Ihn, M. Tsuji, A. Kawaguchi and K. Katayama, *Bull. Inst. Chem. Res., Kyoto Univ.*, **68**, 30 (1990).
(24) K. J. Ihn, M. Tsuji, S. Isoda, A. Kawaguchi and K. Katayama, *Macromolecules*, **23**, 1788 (1990).
(25) T. Trzebiatowski, M. Dräger and G. R. Strobl, *Makromol. Chem.*, **183**, 731 (1982).
(26) K. J. Ihn, M. Tsuji, S. Isoda, A. Kawaguchi, K. Katayama, Y. Tanaka and H. Sato, *ibid.*, **190**, 837 (1989).
(27) p.184 (Fig. III.12) in Ref.2.
(28) p.196 (Fig. III.13) in Ref.2.
(29) Poster presentations at 1st Pacific Polym. Conf., Maui, (1989) and at IUPAC 33rd Int. Symp. Macromol., Montreal (1990).
(30) M. Tsuji, A. Uemura, M. Ohara, A. Kawaguchi, K. Katayama and J. Petermann, *SEN-I GAKKAISHI*, **42**, T-580 (1985); M. Tsuji, A. Uemura, M. Ohara, S. Isoda, A. Kawaguchi and K. Katayama, *Ann. Rep. Res. Inst. Chem. Fibers, Japan*, **44**, 1 (1987).
(31) M. Tsuji, A. Kawaguchi, K. Katayama and K. J. Ihn, *Polym. Prepr., Japan*, **40**, 3913 (1991).
(32) K. Katayama, M. Tsuji, A. Kawaguchi, K. J. Ihn and H. Kawamura, *Ann. Rep. Res. Inst. Chem. Fibers, Japan*, **48**, 75 (1991).
(33) R. Kitamaru, F. Horii and K. Murayama, *Macromolecules*, **19**, 636 (1986).
(34) R. Patil and D. H. Reneker, *Polymer*, **35**, 1909 (1994).
(35) I. Ohki, A. Takahara and T. Kajiyama, *Polym. Prepr., Japan*, **43**, 3913 (1994).
(36) R. Nisman, P. Smith and G. J. Vancso, *Langmuir*, **10**, 1667 (1994).
(37) F. Lin and D. J. Meier, *ibid.*, **10**, 1660 (1994).
(38) R. S. Davé and B. L. Farmer, *Polymer*, **29**, 1544 (1988).